

KfK 4889
Mai 1992

Fuel Equation of State Data for Use in Fast Reactor Accident Analysis Codes

E. A. Fischer
Institut für Neutronenphysik und Reaktortechnik
Projekt Nukleare Sicherheitsforschung

Kernforschungszentrum Karlsruhe

KERNFORSCHUNGSZENTRUM KARLSRUHE
Institut für Neutronenphysik und Reaktortechnik
Projekt Nukleare Sicherheitsforschung

KfK 4889

Fuel Equation of State Data for Use in Fast Reactor
Accident Analysis Codes

E.A. Fischer

Kernforschungszentrum Karlsruhe GmbH, Karlsruhe

Als Manuskript gedruckt
Für diesen Bericht behalten wir uns alle Rechte vor

Kernforschungszentrum Karlsruhe GmbH
Postfach 3640, 7500 Karlsruhe 1

ISSN 0303-4003

Abstract

A new evaluation of the equation of state of urania between the melting point and the critical point was carried out in 1986. The purpose of the work presented in this report is to make these data available for fast reactor accident analysis codes. The basic procedure is to produce analytic data fits for the liquid fuel (i.e. for densities larger than the critical value); for the vapor states (i.e. densities below critical) a suitably modified Redlich-Kwong equation is proposed. A reference analytic representation was produced, which closely fits the evaluated data. Furthermore, suitable approximations to the new data for the codes SIMMER-II, KADIS, and SAS4A were suggested and in part implemented into the codes.

Brennstoff-Zustandsgleichung für Codes zur Analyse von Störfällen in Schnellen Reaktoren

Zusammenfassung

Eine Neuauswertung der Zustandsgleichung für UO_2 zwischen dem Schmelzpunkt und dem kritischen Punkt wurde im Jahr 1986 durchgeführt. In dem vorliegenden Bericht wird beschrieben, wie diese neuen Daten für Störfall-Codes verfügbar gemacht werden. Das Verfahren besteht darin, analytische Anpassungen für den flüssigen Brennstoff (d.h. für Dichten über der kritischen) zu produzieren; für die Dampf-Zustände (d.h. für Dichten kleiner als die kritische) wird eine geeignet modifizierte Redlich-Kwong-Gleichung benutzt. Eine Referenz-Anpassung wurde produziert, die die ausgewerteten Daten mit guter Genauigkeit approximiert. Außerdem wurden geeignete Näherungen für die verschiedenen Störfall-Codes SIMMER-II, KADIS und SAS4A vorgeschlagen und teilweise in die Codes eingebaut.

Table of Contents

	Page
Abstract	
1. Introduction	1
2. The Reference Analytic Representation of the Equation of State above the Melting Point	3
2.1 Two-Phase Region and Compressed Liquid	4
2.2 Superheated Vapor	8
2.3 Supercritical Region	11
2.4 Results and Discussion	13
2.5 Behaviour Near the Critical Point	14
2.6 Entropy of the Saturated Liquid	16
3. Properties of Solid Fuel	19
4. Use of Equation of State in Accident Analysis Codes	21
4.1 General Simplifications	21
4.2 Equation of State for SIMMER-II	21
4.3 Equation of State for the KADIS Code	24
4.4 Equation of State for the SAS Code	27
5. Summary and Conclusions	29
References	30
Appendix	33
Table I	35
Figures	

1. Introduction

A new evaluation of the equation of state (EOS) of urania was carried out in 1986, and published in Ref. [1, 2]. The purpose of this evaluation was to provide reliable EOS data for the analysis of hypothetical core disruptive accidents in fast reactors. The Significant Structures Theory (SST) of liquids was used, but it was extended to the case of non-stoichiometric liquid material, and to a multicomponent vapor phase which consists of the species UO , UO_2 , UO_3 , and oxygen. Only this extended theory provides an adequate description of the urania system. The model parameters were fitted to experimental results which became available in the past decade [3, 4, 5, 6]. In general, good agreement with the experimental data could be obtained using physically reasonable model parameters. The evaluation also involved an extrapolation to the critical point. The predicted critical temperature is 10 600 K, the critical density is 1560 kg/m^3 . The pressure of the uranium-bearing species at the critical point is 158 Mpa, which gives a reasonable value, 0.310, for the critical compressibility. The uranium-bearing species are in equilibrium with an oxygen pressure of 230 Mpa at the critical point, so that the total pressure at the critical point amounts to 388 Mpa. These data certainly deserve more confidence than earlier evaluations, for once because they imply an extrapolation of recent and reliable experimental data, but also because the extended model includes non-stoichiometry effects which are important in the urania system at high temperatures.

The present report deals with making the new EOS available for fast reactor core disruptive accident analysis codes. We have in mind the code SAS4A [7], which is used in different laboratories to analyze the initiation phase of core disruptive accidents. This latest SAS code version is presently replacing the older version, SAS3D. The coupled neutronics-fluid dynamics code SIMMER-II, which was developed at Los Alamos [8], was designed to analyze the transition phase of core disruptive accidents. A more advanced version, SIMMER-III, is presently under developments at the PNC company in Japan. Furthermore, the disassembly code KADIS [9] is still occasionally used at KfK to study energetic power excursions in fast reactors. Each of these codes uses a different analytic format for the EOS, so it seems to be necessary to suggest separate analytic fits for the different codes. Besides, it seems to be appropriate to suggest an extension of the format in certain cases, to allow for better approximations. In principle, EOS data can be used in accident analysis codes either in the form of analytic fits, or in tabular form. The present work concentrates on producing analytic fits, mainly because this is what the above mentioned reactor

codes require. The first fits were proposed as early as 1986 [1]; in the meantime they were refined especially in the vicinity of the critical point. Note that one wants a format for the EOS data in an accident code which, on one side, is simple enough to keep the code running time in reasonable limits, but on the other side is accurate enough to produce physically meaningful results. In the following section, we first present a set of accurate analytic fits to the evaluated data, which can be used as a reference. The application to the above mentioned accident analysis codes is then discussed in the later sections. Note that certain simplifications are necessary when the new EOS is introduced in accident analysis codes. As was pointed out in [1, 2], the data for liquid UO_2 should also be used for the fast reactor mixed oxide fuel, (U, Pu) O_2 .

2. The Reference Analytic Representation of the Equation of State above the Melting Point

The following analytic representation of the UO_2 EOS approximates the evaluation with the Significant Structures Theory very closely. It is available in a computer routine EOSPL 90, which calculates the pressure and the internal energy as functions of the density, with the temperature as a parameter. The lowest temperature is at the melting point, $T_m = 3120$ K. The original SST evaluation was carried out for different oxygen to metal (O/M) ratios, i.e. for different x values in $\text{UO}_{2\pm x}$. The fits, however, were produced only for the stoichiometric case. It was felt that this is accurate enough for accident analysis. The dependence of the vapor pressure on the O/M of the liquid is significant only in the lower temperature range (of liquid $\text{UO}_{2\pm x}$), where the pressure is low anyway. In this work, piecewise polynomial fits will be provided for the "liquid side", i.e. for densities larger than the critical density ($\rho > \rho_c$). For the gas side ($\rho < \rho_c$), the physics based EOS by Redlich and Kwong [10] was suitably modified [11] to approximate the SST data. The reason for this double approach is that in the liquid range, the important functions, e.g. the saturation density or the internal energy, vary smoothly and only by relatively small factors (less than an order of magnitude), so that good accuracy can be obtained with polynomial fits. On the other hand, the gas density varies by several orders of magnitude between the critical density and low gas densities around the boiling point, where the ideal gas law is valid. Therefore, an equation based on a simple physics model was preferred in this range.

While polynomial fits can in principle be obtained with any desired accuracy, the present approach involves already two approximations. One is that the extrapolation into the compressed liquid range is performed with the assumption that the specific heat C_v depends only on density, not on the temperature. This seems to be accurate enough for the usual fluid dynamics and reactor applications, where pressures are low or moderate, and highly compressed liquids do not occur.

The second approximation is the use of the modified Redlich-Kwong EOS, which in connection with the vapor pressure curve determines the saturated vapor density. It was, however, found that for UO_2 the density agrees well enough with the vapor density obtained from SST.

Different analytic approximations are used in the different regions:

- Two-phase region
- Compressed liquid
- Superheated vapor
- Supercritical region.

2.1 Two-Phase Region and Compressed Liquid

The two-phase region is the most important one for accident analysis. The data needed are the vapor pressure, and both the densities and internal energies of the saturated liquid and vapor. Analytic fits were produced for these state variables. Note, however, that a complication arises when a consistent thermodynamic treatment of the uranium/oxygen system is used. Then there is a partial pressure of atomic oxygen (molecular oxygen can be neglected), which is in equilibrium with both the liquid uranium and the mixture of uranium-bearing vapor species (UO, UO₂, UO₃). The pressure of the uranium-bearing species will also be called the saturation pressure, p_s . The reason for choosing this nomenclature is the following: The uranium-bearing vapor mixture in equilibrium with the liquid is said to be at saturation. Thus, its density is called the "vapor saturation density", and it seems appropriate to label the associated pressure the saturation pressure. It is connected with the temperature and the vapor density by a real-gas equation of state, chosen in the present work as a modified Redlich-Kwong-EOS. Besides, certain thermodynamic relations, e.g. the Clausius-Clapeyron equation, clearly involve only the saturation pressure.

On the other hand, the pressure of the uranium system in a two-phase state, in thermodynamic equilibrium, is the sum of the saturation pressure and the oxygen pressure. It will be called the "total pressure". It can be assumed that the components of boiling fuel are in thermodynamic equilibrium, during the temperature transients in a core disruptive accident, so that the total pressure is the one which drives core disassembly in accidents, and which is also seen by the measuring devices in experiments, e.g. the pressure transducer in an in-pile pressure measurement. Therefore, one should in principle use the total pressure in accident analysis codes.

The state variables for the compressed liquid are obtained as follows: The specific heat C_v is obtained from the SST for the saturated liquid. It is assumed that it de-

depends, in good approximation, only on the density, not on the temperature. Thus, for given ρ and T , one needs the saturation temperature T_s , and C_v at the saturation point. The internal energy of the compressed liquid is then (s refers to saturation)

$$U(T, \rho) = U_s(\rho) + C_v(T - T_s) \quad (1)$$

When calculating the pressure of the compressed liquid, one must make sure to satisfy the thermodynamic relation

$$\frac{\partial U}{\partial V} = T \frac{\partial p}{\partial T} - p \quad (2)$$

This requirement leads to the equation

$$p(T, \rho) = p_s(\rho) + \gamma_s(T - T_s) - \rho^2 \frac{dC_v}{d\rho} \left(T \ln \frac{T}{T_s} - T + T_s \right) \quad (3)$$

where the pressure-temperature coefficient γ is defined as the derivative $\partial p / \partial T$ at constant density. In eq. (3), γ_s is γ taken on the saturation line. To obtain this quantity, we apply the relation (2) to a state on the saturation line. This leads to the equation

$$T_s \gamma_s - p_s = \rho^2 \left(- \frac{dU_s}{d\rho} + C_v \frac{dT_s}{d\rho} \right) \quad (4)$$

where the derivatives of U_s and T_s on the right hand side are along the saturation line. In the following, total derivatives will be used for the quantities on the saturation line because they depend only on one independent variable.

Eq. (3) gives only the pressure of liquid urania, and does not include the oxygen pressure. However, to describe saturated states in thermodynamic equilibrium, the pressure should be the total pressure, i.e. the sum of the liquid pressure, and the oxygen pressure. It is, however, not obvious how the oxygen part of the pressure can be extrapolated into the compressed liquid state. The simplest way, which will be used here, is to replace $p_s(\rho)$ in eq. (3) by the total two-phase pressure, $p_t(\rho)$ and keep the other terms as they are in eq. (3). As the liquid is compressed, the pressure increases rapidly beyond the two-phase pressure, and thus this simple approach is completely adequate.

The analytic fits used for the two-phase region and for the compressed liquid are:

- Saturation pressure (of the U-bearing species)

$${}^{10}\log p_s \text{ (Mpa)} = 39.187 + 0.1921 \times 10^{-3} T - 34715/T - 3.8571 \ln T \quad (5)$$

- Total pressure (including oxygen)

$${}^{10}\log p_{\text{tot}} \text{ (Mpa)} = 47.287 + 0.3615 \times 10^{-3} T - 36269/T - 4.8665 \ln T \quad (6)$$

- Saturation temperature and liquid C_v as a function of the liquid density

- a) $2.54 < \rho < 8.86 \text{ (g/cm}^3\text{)}, T_m < T_s < 9951.66 \text{ K}$

$$T_s = 3120 + (8.86 - \rho)/0.916 \times 10^{-3} - 1.7 (8.86 - \rho)^2 \quad (7)$$

$$C_v = 0.2925 + 0.018959 (8.86 - \rho) - 0.0038921 (8.86 - \rho)^2 \\ + 0.5834 \times 10^{-4} (8.86 - \rho)^3 \quad (8)$$

- b) $\rho_c < \rho < 2.54 \text{ (g/cm}^3\text{)}, \text{ or } 9951.66 \text{ K} < T_s < T_c$

$$T_s = 10600 - 427.13 (\rho - 1.56)^2 - 1120 (\rho - 1.56)^3 \\ + 1242.5 (\rho - 1.56)^4 - 365.1 (\rho - 1.56)^5 \quad (9)$$

$$C_v = 0.2597 + 0.010195 (\rho - 1.56) + 0.01134 (\rho - 1.56)^2 \quad (10)$$

In these equations, T_s is in K, ρ in g/cm^3 , C_v in J/gK . The subscript c refers to the critical point, T_m is the melting temperature.

The pressure-temperature coefficient $\gamma = (\partial p/\partial T)_\rho$ on the saturation line can be obtained using the thermodynamic relation, eq. (4). At the critical point, $\gamma = 0.05227 \text{ Mpa/K}$.

Note that the analytic fits for the variables needed in eq. (4) produce a smooth behavior of the pressure-temperature coefficient in the vicinity of the critical point; the only minor weakness is that the slope of the function $\gamma_s(\rho)$ is not monotonous.

This minor inconsistency can be accepted in the range near the critical point, where data are extrapolated, and not well known anyway.

- Internal energy of the saturated liquid U_s (in J/g)

a) In the range $U_m \leq U \leq 4271.0$ (J/g)

or $T_m \leq T_s \leq 9000$ K, the reference relation gives the saturation temperature T_s as a function of U

$$T_s(U) = 3120 + 2.1129 X - 1.4570 \times 10^{-4} X^2 + 4.2737 \times 10^{-8} X^3$$

$$X = U - U_m \quad (11)$$

The internal energy at the melting point is $U_m = 1398.6$ J/g, see Ref. [12]. This relation cannot be inverted analytically. However, an approximate inversion is

$$U_s = 1398.6 + 0.47419 Y + 1.6387 \times 10^{-5} Y^2 - 2.3762 \times 10^{-9} Y^3$$

$$Y = T - T_m \quad (12)$$

For given temperature, eq. (12) can be used to find an approximate value for U_s , which can then be improved by iterating on eq. (11). As long as the temperature is well below critical, the specific heat C_p (at constant O/M) is given by the derivative

$$C_p = \frac{dU_s}{dT} \quad (13)$$

Near the melting point, C_p from equation (13) is close to the value 0.485 J/gK, which was recommended both by Fink et al. [12], and by Rand et al. [13].

b) Internal energy above 9000 K

The use of the Redlich-Kwong equation (see Section 2.2) for $\rho < \rho_c$, and the above data fit for $T_s(\rho)$ require that in the vicinity of the critical temperature, $U_s(T_s)$ must be of the form (see below)

$$U_c - U_s = \left(\frac{T_c - T}{\text{const}} \right)^{1/2} \quad (14)$$

where the constant must be suitably chosen. However, this equation holds only in the immediate neighborhood of the critical point. Therefore, the range 9000 K to T_c was again subdivided; in the lower part, $T < 9780.38$ K, the following equation was obtained

$$T_s = 9000 + 2.3334 (U - 4271) \quad \left\{ \begin{array}{l} 4271 \leq U \leq 4605.44 \\ \text{which corresponds to} \\ 9000 \leq T_s \leq 9780.38 \end{array} \right. \quad (15)$$

In the upper part, close to the critical point, it was preferred to define U_s as a function of $\Delta\rho = \rho - \rho_c$, rather than of the temperature. This way, a polynomial fit is possible, and the square root appearing in eq. (14) is avoided. One has

$$U_s = U_c - 162.82 \Delta\rho - 100 (\Delta\rho)^2 - 188 (\Delta\rho)^3 + 162.96 (\Delta\rho)^4 - 35.62 (\Delta\rho)^5 \quad (16)$$

This relation holds for $\rho < 2.7$ g/cm³, or $T_s > 9780.38$ K.

Note that $U_c = 4992.9$ J/g. The analytical fits for the different regions have the same derivatives at their respective boundaries.

To obtain the state variables in the compressed liquid, one proceeds as follows: First, for a given value of the density ρ (or molar volume V), one finds the saturation temperature T_s , pressure p_s , and internal energy U_s , as well as C_v and dp/dT . The internal energy and the pressure are then obtained from the equations (1) and (4).

2.2 Superheated Vapor

On the vapor side, the EOS must be valid for density variations by several orders of magnitude, between high temperature saturated vapor, where real gas effects are important, and the dilute gas which obeys the ideal gas law. Polynomial fits are not suitable, and it was decided to work with the semi-empirical EOS developed by Redlich and Kwong [10]. As mentioned by Mistura et al. [14], this EOS is widely used for extrapolating thermodynamic data, especially in the chemical industry, and it is quite accurate in the critical region. It was, however, observed earlier [11] that the Redlich-Kwong (RK) EOS had to be modified to be used for UO_2 (and also

for other materials). The modification suggested is fairly obvious, and it is interesting to see that Eberhard, in a recent publication [15], used exactly the same modifications. The RK-EOS reads

$$p = \frac{RT}{V - b} - \frac{a}{T^{1/2} V (V + b)} \quad (17)$$

where $V = 1/\rho$ is the specific volume (or the molar volume; in this report, the specific volume is used). Eq. (17) is a two-parameter EOS, and it is easy to see that this equation implies the following value of the critical compressibility

$$Z_c = \frac{p_c V_c}{RT_c} = 0.332 \quad (18)$$

which is valid for simple liquids. On the other hand, the critical compressibility of UO_2 , as predicted by the SST, is $Z_c = 0.310$. To make the RK-EOS suitable for Z_c different from 0.332, it was modified as follows

$$p = \frac{RT}{V - b_1} - \frac{a(T)}{V(V + b_2)} \quad (19)$$

where $a(T)$ is the function

$$a(T) = a_c (T/T_c)^n \quad (20)$$

Eqs. (19, 20) define a four-parameter EOS. To determine the parameters, we observe that the critical point is defined by the conditions

$$\left(\frac{\partial p}{\partial V} \right)_c = - \frac{RT}{(V - b_1)^2} + \frac{a(T)}{b_2} \left(\frac{1}{V^2} - \frac{1}{(V + b_2)^2} \right) = 0 \quad (21)$$

$$\left(\frac{\partial^2 p}{\partial V^2} \right)_c = \frac{2 RT}{(V - b_1)^3} - \frac{2 a(T)}{b_2} \left(\frac{1}{V^3} - \frac{1}{(V + b_2)^3} \right) = 0 \quad (22)$$

where T, V, p have their critical values. Making the substitutions

$$b_1 = b_{10} V_c, \quad b_2 = b_{20} V_c, \quad a_c = a_0 V_c RT_c,$$

one finds after some simple manipulations that three out of the four parameters, namely b_{10}, b_{20} , and a_0 , are determined by the critical compressibility Z_c .

One obtains for $Z_c = 0.310$

$$\left. \begin{aligned} b_1 &= 0.2204 V_c \quad , & b_2 &= 0.446 V_c \\ a(T_c) &= 1.4065 V_c RT_c \end{aligned} \right\} \quad (23)$$

We now observe that the eqs. (19, 20) in combination with the saturated vapor pressure curve, eq. (5), determine the specific volume of the saturated vapor, V_v . The remaining parameter, namely the exponent n , can then be used to obtain the best fit of V_v with the data given by the SST. This leads to the selection $n = 0.2$, i.e.

$$a(T) = a_c (T/T_c)^{0.2} \quad (24)$$

The internal energy of vaporization is then be defined as

$$\Delta U_{\text{evap}} = \left(T \frac{dp}{dT} - p \right) (V_v - V_l) \quad (25)$$

where V_v and V_l refer to the saturated vapor and liquid. Using the relation (2) one obtains the internal energy of the superheated vapor as a function of T and V

$$U(T, V) = U_s(T) + \Delta U_{\text{evap}} + \frac{(1-n)a(T)}{b_2} \ln \frac{V(V_v + b_2)}{V_v(V + b_2)} \quad (26)$$

Note that the pressure in the equations (17) to (22) is the pressure of the uranium-bearing species only. The total pressure, including the oxygen pressure, at the saturation density is

$$p_t = \frac{RT}{V_v - b_1} - \frac{a(T)}{V_v(V_v + b_2)} + (p_{\text{tot}} - p_s) \quad (27)$$

where p_{tot} and p_s are given by the equations (5, 6). In the superheated vapor regime, one could in principle obtain (for given T) a density dependent equilibrium between the different species, UO , UO_2 , UO_3 , and oxygen, assuming that O/M is constant, and taking account of real-gas effects. This was not done in the present work. Rather, an approximation was used where oxygen behaves like an ideal gas for large volumes, but the tangent $(\partial p/\partial \rho)_T$ is zero at the critical point; i.e.

$$p_o(T, V) = \frac{(p_{\text{tot}}(T) - p_s(T))}{1 - \alpha} \left(\frac{V_v}{V} - \frac{1}{3} \left(\frac{V_v}{V} \right)^3 \right) \quad (28)$$

for $V > V_v$ where α is defined as

$$\alpha = \frac{1}{3} \left(\frac{V_c}{V_v} \right)^2 \quad (29)$$

The total pressure is then

$$p_t = \frac{RT}{V - b_1} - \frac{a(T)}{V(V + b_2)} + p_o(T, V) \quad (30)$$

As mentioned above, V_v is determined through the equations (5), (19), (20). An approximate value for V_v can be obtained from the analytic fit

$$\frac{V_c}{V_v} = \begin{cases} \exp(-0.25 - 0.55 y - 0.241 \times 10^{-3} y^5) & 4000 < T < 10085 \text{ K} \\ 1 - (0.3318 y)^{1/2} & 10085 \text{ K} < T < T_c \end{cases} \quad (31)$$

where

$$y = \frac{T_c - T}{1000}$$

This relation can be used as a first guess for an iterative solution of eqs. (5, 19, 20). If less accuracy is required, eq. (31) can be used directly.

2.3 Supercritical Region

Clearly there is no true theoretical, let alone experimental, information about supercritical UO_2 . Therefore, the following extrapolation can only provide a physically reasonable continuation, which is consistent with the equations for the compressed liquid for densities higher than the critical one, and with the gas equations for densities lower than ρ_c .

For $V < V_c$, the equations (1) and (3) are extrapolated directly into the supercritical region, $T > T_c$, assuming that C_v and γ_s are independent of temperature. For

$V > V_c$, the equations (19) and (30) are used for the pressure. Although it might be desirable to have the same equation over the whole range of V , it was decided to use the mentioned procedure in order to obtain continuity along isochores. Besides, the modified RK equation is not valid if V is very small ($V < b_1$).

The equation for the internal energy for $V > V_c$ is similar to eq. (26). It reads

$$U(T, V) = U_c + C_v (T - T_c) + \frac{0.8 a(T)}{b_2} \ln \frac{V(V_c + b_2)}{V_c(V + b_2)} \quad (32)$$

where C_v has to be taken at the critical density.

In the supercritical region, $a(T)$ is no longer given by Eq. (20), but must be determined from the requirement that the equations (3) and (19) give the same $p(T, V_c)$ at the critical specific volume. This condition reads

$$\frac{a(T) - a_c}{V_c(V_c + b_2)} = \left[\frac{R}{V_c - b_1} - \gamma_c \right] (T - T_c) - \rho_c^2 \frac{dC_v}{d\rho_c} \left[T \ln \frac{T}{T_c} - T + T_c \right] \quad (33)$$

for $T > T_c$.

Thus, $a(T)$ is given by different expressions for $T > T_c$. Note, however, that da/dT must be continuous at T_c , because otherwise $(\partial p/\partial T)_V$ would not be continuous. This can be seen by differentiating eq. (19). This poses an additional condition, which can be written

$$\gamma_c = \left(\frac{dp}{dT} \right)_{T_c} = \frac{R}{V_c - b_1} - \frac{0.2 a_c}{T_c V_c (V_c + b_2)} \quad (34)$$

When the parameters are inserted, the right hand side is equal to 0.05227 Mpa/K. Though the original SST evaluation gave a slightly larger value, the fit in eq. (4) was adjusted in the vicinity of the critical temperature such as to fulfill the requirement (34).

2.4 Results and Discussion

The results for the internal energy, the total pressure, and the pure urania pressure, as obtained by the routine EOSPL90, are shown in Fig. 1, 2 and 3. They are valid if the temperature is at or above the melting temperature (3120 K), and for densities up to and slightly above the liquid density at melting (8.86 g/cm³). These data seem to be the most reliable ones at the present time, because they are based on recent and reliable experimental results.

Fig. 4 and 5 show the evaluated pressure curve in the 2-phase region, and the comparison with experimental data. They were already published in [1], but are reproduced here for the reader's convenience. Fig. 4 shows the total pressure as a function of temperature up to 5000 K. In this range, the evaluated saturation pressure (i.e. pressure of the U-bearing species) is only slightly lower than the total pressure; the difference amounts to about 9 % at 5000 K. Fig. 5 shows both the total and saturation pressure (p_t and p_{sat}) at still higher fuel enthalpy. For easy comparison with the In-pile experiments [3, 4] the fuel enthalpy is used as the variable. Note that p_t and p_{sat} are both within the error limits of the experiments. At the highest enthalpy reached in the experiments (~ 3700 J/g), the difference between p_t and p_{sat} amounts to a factor of 1.5.

The fits for the variables in the liquid state (internal energy, density, and C_v) were improved at high temperatures, especially in the vicinity of the critical point, since the first evaluation was published [1]. The present equations provide good thermodynamic consistency, and they also approximate the SST data more accurately than those given in [1].

The program EOSPL90 calculates also the temperature derivatives C_v and dp/dT . The equations are obtained in a straightforward manner from the equations in this report, and there is no need to explicitly write them down here.

To discuss the data at the melting point, we use the relation

$$C_p = C_v + \frac{T\alpha^2}{\rho\beta} \quad (35)$$

where the specific heats are in J/gK, α is the liquid volume expansion coefficient, and β the isothermal compressibility (cm³/J). The SST gives the following data at the melting point:

$$C_v = 0.2925 \text{ (J/gK)} \quad , \quad \alpha = 1.051 \cdot 10^{-4} \text{ (K}^{-1}\text{)}$$

$$C_p = 0.480 \text{ (J/gK)} \quad , \quad \beta = 2.07 \times 10^{-5} \text{ (cm}^3\text{/J)}$$

$$\rho = 8.86 \text{ (g/cm}^3\text{)} \quad T_m = 3120 \text{ K}$$

Note that the derivatives C_v , C_p , α and β were revised by a few percent as compared to the data in [1]. There is a rather large difference $C_p - C_v$. While C_v has the value 9.5 R, which is about normal for a 3 atomic molecule, $C_p = 15.59$ R is unusually large. It is, however, consistent with both the evaluations by Fink et al. [12], and by Rand et al. [13]. Both groups suggest $C_p = 0.485$ J/gK based on experimental data. In addition, the thermal expansion coefficient α is also well in agreement with evaluations and experiment [12, 13]. The compressibility β , however, is significantly lower than the value measured by Slagle and Nelson [16]. The experiment gave 3.6×10^{-5} cm³/J for the adiabatic compressibility; using known values of C_p and α , one estimates 4.4×10^{-5} cm³/J for the isothermal compressibility, to be compared with the SST result of 2.07×10^{-5} cm³/J.

Combining the experimental value with C_p and α in eq. (35) leads to $C_v = 12.7$ R. This high value indicates that the "excess heat capacity" observed in solid UO₂ near the melting point should also be present in the liquid. The excess heat capacity in the solid is attributed to the formation of Frenkel defects or to electronic disorder, or most likely to both of them [17]. It is not clear a priori how these phenomena should be extrapolated into the liquid. The experimental data, inasfar as they are reliable, indicate that there is an excess heat capacity in the liquid state also. The SST, which does not model an increased heat capacity, gives a high C_p value due to the low compressibility. This is certainly a weakness in the present model.

2.5 Behaviour Near the Critical Point

Some effort was needed to arrive at polynomial fits for the liquid in the vicinity of the critical point, which reproduce the SST data with adequate accuracy, provide thermodynamic consistency, and a smooth joining to the Modified Redlich-Kwong EOS on the gas side. Note that at supercritical temperatures, the separation line between the two different representations is the critical isochore. To show the result, the internal energy and the two pressure variables (total pressure and pressure of the U-bearing species) are shown, as functions of temperature and density,

in the vicinity of the critical point (Fig. 6, 7, 8). It is obvious that smooth behaviour of these functions could be reached. In some instances, however, derivatives show a small jump (typically < 5 %) instead of being continuous. It was not considered high priority to remove these small discontinuities. The behaviour of the thermodynamic functions and their derivatives near the critical point will now be explained in more detail.

The physics of phase transitions and critical phenomena as developed in the 1960's and 1970's tells that the so-called "critical exponents" are fractional numbers [18, 19]. Moreover, these exponents are universal numbers, i.e. they are the same for all liquid-vapor transitions. Especially, the exponent of the saturation line is $\beta = 0.325$. On the other hand, the van der Waals equation and equations developed from it are based on a mean-field theory. In this class of equations, the critical exponents are either integers or half integers (e.g. $\beta = 0.5$ for the saturation line). Both the Significant Structures Theory and the Modified Redlich-Kwong EOS belong to the latter class. Therefore, the analytic fits were adjusted such that they reproduce the mean-field critical exponents.

The behavior of the Reference Analytic Representation in the vicinity of the critical point will now be briefly outlined. The quantity ε is defined as

$$\varepsilon = 1 - T/T_c$$

Saturation Line:

The liquid density ρ_l and the vapour density ρ_v are

$$\rho_l/\rho_c - 1 = A_l \varepsilon^{0.5}$$

$$\rho_v/\rho_c - 1 = -A_v \varepsilon^{0.5}$$

The critical exponent is 0.5 as with the van der Waals equation [17, 18], whereas the "universal critical exponent" is 0.325. Note that the coefficients A_l and A_v are not equal.

The Pressure and its Derivatives:

In a mean-field theory, both the saturation pressure and the pressure-temperature coefficient $\gamma = \partial p/\partial T$ are continuous at the critical point, and the exponent along the

critical isotherm is $\delta = 3.0$. Our numerical fits reproduce this behavior rather closely, except that the pressure-temperature coefficient shows a small discontinuity (4.5 %) at the critical point.

The pressure-temperature coefficient γ_s , as calculated from eq. (4), with the data of the Reference Analytic Representation (Fig. 9) is smooth in the vicinity of the critical point; the only minor weakness is that the slope is not monotonous, as mentioned in Section 2.1.

The Internal Energy and its Derivatives:

The specific heat C_v remains finite at the critical point and has the value as produced by the SST, namely $C_v = 0.2597 \text{ J/gK}$. This corresponds to a critical exponent $\alpha = 0$, whereas the universal exponent is $\alpha = 0.11$. In the supercritical region, the derivative $\partial U/\partial \rho$ is connected with γ through the equation

$$\frac{\partial U}{\partial \rho} = \frac{p_s - T\gamma}{\rho^2}$$

This quantity is continuous when the critical isochore is crossed, as must be.

Thus, the behaviour of our Reference Analytic Representation is considered satisfactory.

2.6 Entropy of the Saturated Liquid

In the analysis of the post-disassembly expansion phase, the work potential due to isentropic expansion of the fuel is often used. Therefore, the entropy of both liquid fuel and fuel vapor must be known, with the entropy of the saturated liquid as a key quantity. It can be obtained from the relation

$$dS = \frac{dU}{T} + \frac{pdV}{T} \quad (36)$$

Integrating this equation from the melting point along the saturation line to any liquid temperature, one finds that the first term dU/T , is by far the dominant one, and the second one is just a minor correction.

The range between melting point and critical point is divided into two different regions:

$$\begin{array}{ll} \text{Region 1} & T_m < T_s < 9000 \text{ K} \\ \text{Region 2} & 9000 \text{ K} < T_s < T_c \end{array}$$

The integral of the first (and major) contribution to dS can be written

$$\int \frac{dU}{T_s(U)} \quad (37)$$

This integral can be evaluated analytically for Region 1, using the relation (12). One obtains for the first contribution (in units J/gK).

Region 1:

$$\Delta S_1(T) = 0.302542 \ln(T/T_m) + 7.7256 \times 10^{-5}(T - T_m) - 3.5643 \times 10^{-9}(T^2 - T_m^2) \quad (38)$$

The second contribution,

$$\int \frac{pdV}{T} \quad (39)$$

must be evaluated numerically. High accuracy is not needed because this contribution is small anyway. One obtains

Region 1:

$$\Delta S_2(T) = \exp(-7.1027 - 7.893 \times 10^{-4}x - 1.4014 \times 10^{-7}x^2) \quad (40)$$

$$x = 9000 - T$$

The entropy of the liquid is then

$$S_l(T) = S_m + \Delta S_1 + \Delta S_2 \quad (41)$$

where $S_m = 1.17032 \text{ J/gK}$ is the entropy of the liquid at the melting point, see Section 3. The entropy at 9000 K is then $S_l = 1.69190 \text{ J/gK}$.

In Region 2, the following fit was obtained

$$S_1(U) - S_1(4271.0) = 0.11331 \times 10^{-3} x - 12.908 \times 10^{-9} x^2 + 22.124 \times 10^{-21} x^6 \quad (42)$$
$$x = U - 4271.0$$

Note that eq. (42) defines the entropy as a function of internal energy, not of temperature. The reason is that this function is smooth in the vicinity of the critical point. The value $U = 4271.0$ corresponds to 9000 K.

The entropy S_c at the critical point is then

$$S_c = 1.77010 \text{ J/gK}$$

The entropy of the saturated vapour can then be found easily from the equation

$$S_v = S_l + \frac{\Delta U_{\text{evap}} + p_s (V_v - V_l)}{T} \quad (43)$$

3. Properties of Solid Fuel

The present evaluation is restricted to liquid UO₂. For solid oxide fuel, there are two high-quality property evaluations available, which will be briefly discussed. The thermodynamic properties needed for solid fuel are the enthalpy (which for solid fuel is the same as the internal energy), the entropy, and the density.

First, there is the evaluation for UO₂ published by Fink et al. [12] of ANL. These properties, which have been available for quite a while, were widely used as reference data. They are very similar to the data by Rand et al. [13], that emerged from an IAEA project. Most of the evaluation work for liquid UO₂ presented in this report was performed up to 1989, and the data are normalized such that they are consistent with the Fink et al. results. This is shown by quoting the data at the melting point ($T_m = 3120$ K) for both solid and liquid fuel:

	Solid	Liquid
Internal energy (J/g)	1121.6	1398.6
Entropy (J/gK)	1.0815	1.1703
Density (g/cm ³)	9.65	8.86

The limitation of the Fink et al. evaluation is that they refer to UO₂; no data for mixed oxide are quoted.

Second, a more recent evaluation was carried out in 1989 by Harding et al. at the Harwell Laboratory [20], under contract with the Commission of the European Communities. While their data for the UO₂ enthalpy are close to the Fink et al. results, these authors present an interesting method to obtain the mixed oxide enthalpy by a suitable interpolation between the UO₂ and the PuO₂ data. In addition, the authors discuss the effect of non-stoichiometry and burnup on fuel enthalpy. This evaluation is probably the best available for mixed oxide.

In the following, the equations recommended in Ref. [12], which are consistent with our data, will be quoted. One has for the enthalpy of solid UO₂ for $298.15 < T < 2670$ K:

$$H^{(T)} - H_{298.15} \text{ (J/g)} = \tag{44}$$

$$C_1 \theta \left[\left(e^{\theta/T} - 1 \right)^{-1} - \left(e^{\theta/T^*} - 1 \right)^{-1} \right] + C_2 (T^2 - T^{*2}) + C_3 (T - T^*) \exp(-21841/T)$$

where $\theta = 516.11$ K, $T^* = 298.15$ K, $C_1 = 0.289674$, $C_2 = 1.4302 \times 10^{-5}$, and $C_3 = 108.455$;
and for $2670 < T \leq 3120$ K:

$$H_T - H_{298.15} \text{ (J/g)} = 0.618667 T - 808.67 \quad (45)$$

The entropy of solid UO_2 is given by the equations:
For $298.15 < T < 2670$ K:

$$\begin{aligned} S \text{ (J/gK)} = & 0.11238 + C_1 \left[\frac{\theta}{T} \left(1 + \left(e^{\theta/T} - 1 \right)^{-1} \right) - \ln \left(e^{\theta/T} - 1 \right) \right] \\ & + 2 C_2 T + C_3 \left[1 - \frac{T^*}{21841} \left(\frac{21841}{T} + 1 \right) \right] \exp \left(- \frac{21841}{T} \right) \\ & + \exp \left(- 27.6747 + 0.013281 T - 1.8925 \times 10^{-6} T^2 \right) \end{aligned} \quad (46)$$

and for $2670 < T < 3120$ K

$$S \text{ (J/gK)} = 0.98518 + 0.618667 \ln(T/2670) \quad (47)$$

The theoretical density of solid UO_2 ($298.15 < T < 3120$ K) is

$$\rho \text{ (g/cm}^3\text{)} = 10.970 (1.0056 - 1.6324 \times 10^{-5} T - 8.3281 \times 10^{-9} T^2 + 2.0176 \times 10^{-13} T^3) \quad (48)$$

Note that the equations for the enthalpy given in the Journal of Nuclear Materials and in ANL-CEN-RSD-82-3 [12] are not identical, though numerically they agree to at least four significant figures. The equation quoted here is from the Journal of Nuclear Materials, and is consistent with the equation for the entropy.

4. Use of Equation of State in Accident Analysis Codes

4.1 General Simplifications

As explained earlier, the pressure over liquid UO_2 is composed of the pressure of the uranium-bearing species (called "saturation pressure" in this report) and of the oxygen pressure. The fact that both partial pressures show different dependence on the variables, and that the thermodynamic relations involve the saturation pressure rather than the total pressure means that the equations are more complex than is desirable for accident analysis codes. It is, therefore, suggested to use the saturation pressure in these codes, though the total pressure would be more realistic. As discussed in Section 2 (Fig. 5), the difference becomes important only at extremely high temperatures. This means a significant simplification on the gas side because p_0 in eq. (28) is set to zero. Besides, a somewhat simplified set of equations for the liquid side is given in Appendix A. It can be used whenever data at extremely high temperatures ($> 2/3 T_c$) are unimportant, or do not require good thermodynamic consistency.

4.2 Equation of State for SIMMER-II

The analytic EOS in SIMMER-II is strongly simplified [8]. Especially, the saturated vapor pressure is represented by a two-parameter curve,

$$\ln p_s = \ln p^* - \frac{T^*}{T} \quad (49)$$

with the two parameters p^* and T^* ; the specific heat of the solid is assumed constant, and the equations used for the gas-side EOS do not represent real-gas effects very well.

An effort was made [21] to replace the gas-side EOS in SIMMER-II by the modified Redlich-Kwong EOS. However, the other simplifications remain. Therefore, this Section will address the standard SIMMER-II version, and present a set of fuel EOS input data which are recommended for use with fuel typical of SNR-300. Some of

the data are interrelated and these relations will be made clear. The input data set is given in Table I.

While it is common in thermodynamics to normalize the internal energy (or enthalpy) to zero at $T = 298.15$ K, in SIMMER it is normalized to zero at absolute zero. The SIMMER equations are

$$E_{\text{sol}}(T) = C_{\text{VS}} T \quad (50)$$

$$E_1(T) = C_{\text{VS}} T_m + \Delta H_f + C_{\text{VL}}(T - T_m) \quad (51)$$

where ΔH_f is the heat of fusion.

If C_{VS} is determined from the difference in internal energy between 298.15 K and 3120 K (melting point of UO_2), one finds with the data in Section 3

$$C_{\text{VS}} = \frac{1121.6}{3120 - 298.15} = 397.45 \frac{\text{J}}{\text{kg K}}$$

Then one has

$E_{\text{sol}}(T_m)$	1240.0 kJ/kg
ΔH_f	<u>277.0 KJ/kg</u>
$E_1(T_m)$	1517.0 kJ/kg

Adding the difference in internal energy between 3120 K (liquidus of UO_2) and the critical point, $\Delta E = 3594.3$ kJ/kg, one obtains

$$E_{\text{crit}} = 5111.3 \text{ kJ/kg}$$

to be used in SIMMER-II, for UO_2 fuel.

As was mentioned in the introduction, the data for liquid UO_2 should also be used for the fast reactor fuel mixed oxide, $(\text{U}, \text{Pu})\text{O}_2$. In this case, however, the internal energy must be normalized slightly differently because the melting temperature is lower. This is done in a simple consistent manner, which does not account for the slightly different specific heat of mixed oxide. The fuel which was proposed for SNR-300 has a melting temperature of 2977.3 K instead of 3120 K. Retaining C_{VS} and ΔH_f (which is reasonable), one obtains for the internal energy at 3120 K

$E_{\text{sol}} (2977.3)$	1183.3 J/g
ΔH_f	277.0 J/g
$(3120 - 2977.3) C_{VL}$	<u>69.2</u> J/g
	1529.5 J/g

The energy level in the liquid state is 12.5 J/g higher than for pure UO_2 . Therefore, also E_{crit} should be increased by that difference, i.e.

$$E_{\text{crit}} = 5123.8 \text{ kJ/kg}$$

If users of SIMMER-II prefer other data for C_{VS} , C_{VL} , and T_m (e.g. for fuel with a different Pu content), they should make sure to use a value for E_{crit} which is consistent with their data.

A fit of the liquid fuel density in terms of the SIMMER-II parameters was also obtained. The following equations were found for $T < 2/3 T_{\text{crit}}$:

$$\rho_{11} \left(\frac{\text{g}}{\text{cm}^3} \right) = 11.7056 - 0.908018 \times 10^{-3} T - 1.2952 \times 10^{-9} T^2 \quad (52)$$

and for $2/3 T_{\text{crit}} < T < T_{\text{crit}}$

$$\frac{\rho_{12}}{\rho_{\text{crit}}} = 1 + 3.76744 \zeta^{0.65} + 4.53873 \zeta^2 \quad (53)$$

where

$$\zeta = 1 - \frac{T}{T_{\text{crit}}}$$

At $T = 2/3 T_{\text{crit}}$, the two fits have the same value, and the difference in the derivative is only about 5 %.

4.3 Equation of State for the KADIS Code

The Karlsruhe core disassembly code KADIS [9] is similar to VENUS-II [22], which was developed at ANL. The code is still occasionally used for parametric studies. It has a choice of several EOS formulas, but the one that was mostly used is the so-called "ANL-EOS", which was derived by Jackson and Nicholson [22]. It is based on an older evaluation by Menzies [23], and should not be confused with the property data by Fink et al. [12].

The new EOS which is available in the code now involves a progress in different ways: first, the new EOS for liquid fuel is introduced. This means especially that the vapor pressure is lower than the one in the ANL EOS. Second, for solid fuel, the ANL data for the internal energy [12] are used, rather than a constant specific heat. Third, the data for the isentropic expansion are consistent with the ones used for the excursion calculation. The new EOS for KADIS neglects oxygen pressure but otherwise uses the Reference Analytic Representation described in Section 2. In the KADIS code, the independent variables for the EOS are the density and the internal energy; the EOS routine then calculates the temperature and the pressure. In the important case where the fuel is liquid, a mesh cell can be either in a two-phase, or a single-phase state. In the first case, the pressure is the fuel vapor pressure (plus a sodium vapor pressure if a fuel-coolant interaction is modeled), and the temperature is obtained from eq. (11), (15), or by inverting eq. (16). If single-phase liquid pressure occur in a cell, the code calculates pressure equilibrium between the components fuel, steel, and sodium. Single-phase states can occur when the liquid fuel by thermal expansion fills the free volume in a cell, especially during sodium - in accidents, or when a cell is compressed by rapidly expanding neighboring cells. Note that in KADIS single-phase pressures can be calculated erroneously if the sodium density is less than the liquid saturation density.

The EOS routine (subroutine EQUSTA) performs the following calculation. Let ρ be the density of the fuel, smeared over the available free volume in the cell. Calculate the saturation temperatures $T_s(\rho)$, using eqs. (7), (9), and $T_s(U)$ using eq. (11). Then, if $T_s(\rho) > T_s(U)$, the volume required for the fuel to be in a two-phase state is available. Otherwise, the cell is in a single-phase state. The procedure for the two-phase case is as described above. In the single-phase case, the fuel temperature is calculated by solving eq. (3) for the temperature

$$T(U, \rho) = T_s(\rho) + (U - U_s(\rho)) / C_v \quad (54)$$

The eq. (3) for the pressure is used in a simplified form, retaining only the linear term in the fuel temperature

$$p(U, \rho) = p_s(\rho) + \gamma_s (T - T_s(\rho)) \quad (55)$$

In cells where the fuel is still solid, the temperature is obtained by an approximate inversion of U - T relation proposed by the ANL group [12], eq. (44) or eq. (45). The vapor pressure is negligible, and a significant pressure can only occur if the cell becomes single-phase. If fuel is melting in a cell, the temperature rises by 1 K between the solidus and the liquidus, as in the original KADIS code. Again, pressure can only be single phase pressure (caused by the density decrease during melting). The pressure equilibrium between the materials present in the cell is calculated using the compressibility of liquid fuel also for the melting fuel.

These equations were introduced in the EOS subroutine EQUSTA. In addition, the subroutines HYDRIN (initialization) and MOLTU (energy in molten fuel) were modified.

When an energetic power excursion is terminated, the hot fuel, which is under high pressure, expands and loads the structures by conversion of thermal to mechanical energy. KADIS has the capability to calculate the isentropic work energy of the hot fuel during the expansion phase. The method described by Reynolds et al. [24] is used. For this calculation the final state of the KADIS run becomes now the initial state of the expansion phase. The calculation is done independently for each cell which has a pressure higher than the "final" expansion pressure given by input.

The method will be briefly outlined. First one calculates, for each cell, the fuel internal energy U_i and entropy S_i ($i = \text{initial}$). For two-phase cells

$$U_i = U_1 + \Delta U_{\text{evap}} x_i \quad (56)$$

and

$$S_i = S_1 + \Delta S_{\text{evap}} x_i \quad (57)$$

where U_1 , S_1 , ΔU_{evap} , and ΔS_{evap} are functions of the (initial) temperature, and x_i is the initial "vapor quality"

$$x_i = \frac{m_v}{m_1 + m_v}$$

of the fuel. In single-phase cells, only liquid fuel exists, and

$$U_i = U_s + C_v (T - T_s) \quad (58)$$

$$S_i = S_s + C_v \ln (T/T_s) \quad (59)$$

where $T_s = T_s(\rho)$ is the (initial) saturation temperature. The final state is always two-phase, and the "final" vapor quality is obtained from the requirement that the final entropy is equal to the initial entropy. The work potential is then the difference $U_i - U_f$.

For this calculation (routine MECENG in KADIS) the liquid entropy, as given in Section 2.6, is needed.

A comparison calculation was run using the "old" ANL EOS and the new EOS described in this report. The case selected is an energetic disassembly in a reactor of the 300 MWe class. The core is fully voided, the fuel has a temperature distribution, with an average around the melting point. A 21.6 \$/s reactivity ramp is postulated.

The important results are:

	ANL EOS	New EOS
duration of disassembly (ms)	5.52	6.29
thermal energy in the molten fuel (MJ)	3373	3571
mean temperature of the molten fuel (K)	3840	3862
isentropic expansion to 1 bar:		
work energy (MJ)	71.2	98.0
final volume (m ³)	301	419
isentropic expansion to 10 bar:		
work energy (MJ)	11.9	6.6
final volume (m ³)	8.5	4.9

As the new vapor pressure curve is lower than the old one, shutdown takes longer, and the thermal energy in the molten fuel increases. The results for the isentropic expansion show different trends: For the final pressure of 1 bar, the work energy increases by a factor which is larger than the increase in thermal energy. If the final

pressure is 10 bar, the work energy even decreases, so that the increase in the thermal energy is more than compensated during the expansion phase. The main reason for these different trends is the difference in slope between the two vapor pressure curves between 1 and 10 bar, where the new curve is flatter. Therefore, a larger expansion is needed to reach 1 bar. Besides, the Reynolds et al. [24] data used in the older version for the expansion analysis are not fully consistent with the ANL EOS; e.g., the latter uses a constant specific heat, whereas Reynolds et al. proposed a variable specific heat. Thus, the new results are more reliable because the data are consistent, and established by experiments.

4.4 Equation of State for the SAS Code

The code SAS4A is the latest and most advanced one among the SAS codes, that were developed over many years at the Argonne National Laboratory [7]. The SAS codes are used to analyze the initiation phase of core disruptive accidents. SAS4A is at present in a stage of testing and verification at several laboratories in different countries. This procedure should include an updating of the fuel EOS data, and a proposal which data should be used will be given in this Section. Note that SAS can be used for energetic accidents, where the fuel vapor pressure is the mechanism for shutdown, but it cannot calculate single-phase pressures nor motions across the fuel element boxes after thermal or mechanical failure of those.

The following data are suggested:

Fuel enthalpy

- solid fuel: data of Harding et al. [20] for mixed oxide
- heat of fusion: 277 kJ/kg
- liquid fuel: eq. (12), with a slight change in normalization if the fuel is mixed oxide, and the melting point is lower than 3120 K. See Section 4.3

Vapor pressure: eq. (5)

Theoretical density:

- solid fuel: eq. (48)
- liquid fuel:

$$\rho = 8.86 - 0.916 \times 10^{-3}(T - 3120)$$

This is the inversion of eq. (7); the last term is neglected because it is significant only at extremely high temperatures.

It should be mentioned that this proposal was not discussed in detail with the users of SAS4A; thus, difficulties that could arise were not considered, and the suggestion must be considered as tentative.

5. Summary and Conclusions

This report describes how an equation of state for liquid fuel, which was evaluated in 1986, can be made available and used in fast reactor accident analysis codes. The basic procedure is to produce analytic data fits for liquid fuel, (i.e. for densities larger than the critical) and a modified Redlich-Kwong equation for the fuel vapor, (i.e. for densities lower than critical) up to and beyond the critical temperature if needed for parametric studies. A Reference Analytic Representation was produced, which closely fits the evaluated data. In addition, formulations for the codes SIMMER-II and KADIS are prepared and introduced into the codes. It was found by KADIS runs that using the new data, both the thermal energy produced in an excursion, and the isentropic work potential increase. The increase in thermal energy is expected because of the lower vapor pressure curve. The observed increase in the isentropic work potential may be partly due to an inconsistency in the older data. A data set for the code SAS4A is also suggested, and it is expected that it will be used at an appropriate time.

References

1. E.A. Fischer "Evaluation of the Urania Equation of State Based on Recent Vapour Pressure Measurements"
KfK-4084 (1987)
2. E.A. Fischer
Nucl. Sci. Eng. 101, 97 - 116 (1989)
3. R. Limon, G. Sutren, P. Combette, and F. Barbry, "Equation of State of Non-Irradiated UO₂,"
Proc. Topl. Mtg. Reactor Safety Aspects of Fuel Behavior, Sun Valley, Idaho, August 2 - 6, 1981, American Nuclear Society (1981), Vol. 2, page 576
4. W. Breitung and K.O. Reil, "In-Pile Vapour Pressure Measurements on UO₂ and (U, Pu)O₂,"
KfK-3939, Kernforschungszentrum Karlsruhe (1985).
See also Nucl. Sci. Eng. 101, 26 - 40 (1989)
5. M. Bober and J. Singer
Nucl. Sci. Eng., 97, 344 (1987)
6. R.W. Ohse, J.F. Babelot, C. Cercignani, J.P. Hiernaut, M. Hoch, G.J. Hyland, and J. Magill
J. Nucl. Mater., 130, 165 (1985)
7. A.M. Tentner et al. "The SAS4A LMFBR Whole Core Accident Analysis Code"
Trans. International Meeting on Fast Reactor Safety, Knoxville, Tennessee, April 21 - 25 (1985), Vol. 2, page 989
8. L.L. Smith et al. "SIMMER as a Safety Analysis Tool"
Proc. LMFBR Safety Topical Meeting, Lyon, France, July 19 - 23 (1982),
Vol. II, page II-35
9. P. Schmuck, G. Jacobs, G. Arnecke "KADIS: Ein Computerprogramm zur Analyse der Kernzerlegungsphase bei hypothetischen Störfällen in schnellen, natriumgekühlten Brutreaktoren"
KfK 2497 (1977)

10. O. Redlich and J.N.S. Kwong
Chem. Review 44, 233 (1949)
11. E.A. Fischer, Unpublished work (1986)
12. J.K. Fink, M.G. Chasanov, and L. Leibowitz
J. Nucl. Mater 102, 17 - 25 (1981).
See also: J.K. Fink, M.G. Chasanov, and L. Leibowitz: "Properties for Reactor Safety Analysis", ANL-CEN-RSD-82-3 (1982)
13. M.H. Rand, R.J. Ackermann, F. Gronvold, F.L. Oetting, and A. Pattoret
Rev. Int. Hautes Temp. et Refract. 15, 355 (1978)
14. L. Mistura, J. Magill, and R.W. Ohse
J. Nucl. Mater 135, 95 (1985)
15. J.G. Eberhard
"Applying the Critical Conditions to Equations of State"
J. Chemical Education 66, 990 - 993 (1989)
16. O.D. Slagle and R.P. Nelson
J. Nucl. Mater. 40, 349 (1971)
17. K.A. Long, J.F. Babelot, J. Magill, R.W. Ohse, M. Hoch
High Temperatures - High Pressures 12, 515 - 536 (1980)
18. A.L. Sengers, R. Hocken, J.V. Sengers, "Critical Point Universality and Fluids"
Physics Today, Dec. 1977, p. 42
19. H.E. Stanley
Introduction to Phase Transitions and Critical Phenomena
Clarendon Press, Oxford 1971
20. J.H. Harding, D.G. Martin, P.E. Potter
Thermophysical and Thermochemical Properties of Fast Reactor Materials
EUR 12402 EN (1989)

21. E.A. Fischer and S. Kleinheins, Unpublished work (1987)
22. J.F. Jackson and R.B. Nicholson
"VENUS-II, An LMFBR Disassembly Program"
ANL-7951 (1972)
23. D.C. Menzies
The Equation of State of Uranium Dioxide at High Temperatures and Pressures
UKAEA report TRG 1119 (D), 1966
24. A.B. Reynolds
"Fuel Vapor Generation in LMFBR Core Disruptive Accidents"
Nucl. Technol. 26, 165 (1975)

Appendix

A Simplified Analytic Representation of the Equation of State

The following analytic representation is an alternative to the Reference Representation. Both are nearly identical to the up to about 9000 K, except that a separate fit for the pressure-temperature parameter γ_s is given. In the vicinity of the critical temperature, this representation is simplified. Therefore, it is easier to use, but somewhat less accurate. However, for most purposes where the temperatures are significantly below critical, it is practically equivalent to the Reference Analytic Representation.

Analytic fits for the two-phase region and for the compressed liquid:

- Saturation pressure (of the U-bearing species)

$${}^{10}\log p_s \text{ (Mpa)} = 39.187 + 0.1921 \times 10^{-3} T - 34715/T - 3.8571 \ln T$$

- Saturation temperature, liquid C_v and γ_s as a function of the liquid density

- a) $2.1514 < \rho < 8.86 \text{ (g/cm}^3\text{)}, T_m < T_s < 10367.3 \text{ K}$

$$T_s = 3120 + (8.86 - \rho)/0.916 \times 10^{-3} - 1.7 (8.86 - \rho)^2$$

$$C_v = 0.27813 + 0.044561 (8.86 - \rho) - 0.013082 (8.86 - \rho)^2$$

$$+ 9.277 \times 10^{-4} (8.86 - \rho)^3$$

$$\gamma_s = 0.1712 + 0.23474 (8.86 - \rho) - 0.057937 (8.86 - \rho)^2 + 0.028821 (8.86 - \rho)^3$$

- b) $\rho_c < \rho < 2.1514 \text{ (g/cm}^3\text{)}, \text{ or } 10367.3 \text{ K} < T_s < T_c$

$$T_s = 10600 - 427.13 (\rho - 1.56)^2 - 681.118 (\rho - 1.56)^4$$

$$C_v = 0.2597 + 0.023710 (\rho - 1.56) - 0.015218 (\rho - 1.56)^2$$

$$\gamma_s = 0.05227 + 0.3193 \times 10^{-3} (\rho - 1.56)^2 + 0.11184 (\rho - 1.56)^3$$

In these equations, T_s is in K, ρ in g/cm^3 , C_v in J/gK . The subscript c refers to the critical point, T_m is the melting temperature.

Internal energy of the saturated liquid U_s (in J/g)

In the range $U_m \leq U \leq 4271.0$ (J/g)

or $T_m \leq T_s \leq 9000$ K, the saturation temperature T_s is given as a function of U by the equation

$$T_s(U) = 3120 + 2.1129 X - 1.4570 \times 10^{-4} X^2 + 4.2737 \times 10^{-8} X^3$$

$$X = U - U_m$$

Internal energy between 9000 and 10515.5 K

$$T_s = 9000 + 2.3334 (U - 4271) \quad \left\{ \begin{array}{l} 4271 \leq U \leq 4920.48 \\ \text{which corresponds to} \\ 9000 \leq T_s \leq 10515.5 \end{array} \right.$$

Internal energy between 10515.5 K and T_c

$$T_s = T_c - 0.0161125 (4992.9 - U)^2$$

On the vapor side, the modified Redlich-Kwong equation is used, with the same parameters as in Section 2, but omitting the terms for the oxygen partial pressure.

Table I Fuel Equation of State Input for SIMMER-II

Variable	Value		Description
CVS	397.45	J/kg K	specific heat of the solid fuel
TMLT	2977.3	K	melting temperature
HFUS	277000	J/kg	heat of fusion
ROLE	8991	kg/m ³	liquid microscopic density
CVL	485	J/kg-K	liquid-phase specific heat
PSTAR	0.344 x 10 ¹¹	pa	} parameters of the vapor pressure curve
TSTAR	48000	K	
TSUP	20	K	superheat
HSTAR	2.25 · 10 ⁶	J/kg	} parameters of the heat of vaporization equation
ZETA	0.75	-	
TCRIT	10600	K	critical temperature
ROLCRT	1560	kg/m ³	critical density
CVG	300	J/kg-K	gas-phase specific heat at constant volume
GAM	1.10332	-	ratio of constant-pressure specific heat to constant-volume specific heat the vapor phase
ENCRIT	5.11 · 10 ⁶	J/kg	internal energy at the critical point
WTMOL	270	kg/kmol	molecular weight
ROGP95	907.7	kg/m ³	saturated vapor density at T = 0.95 T _{crit}

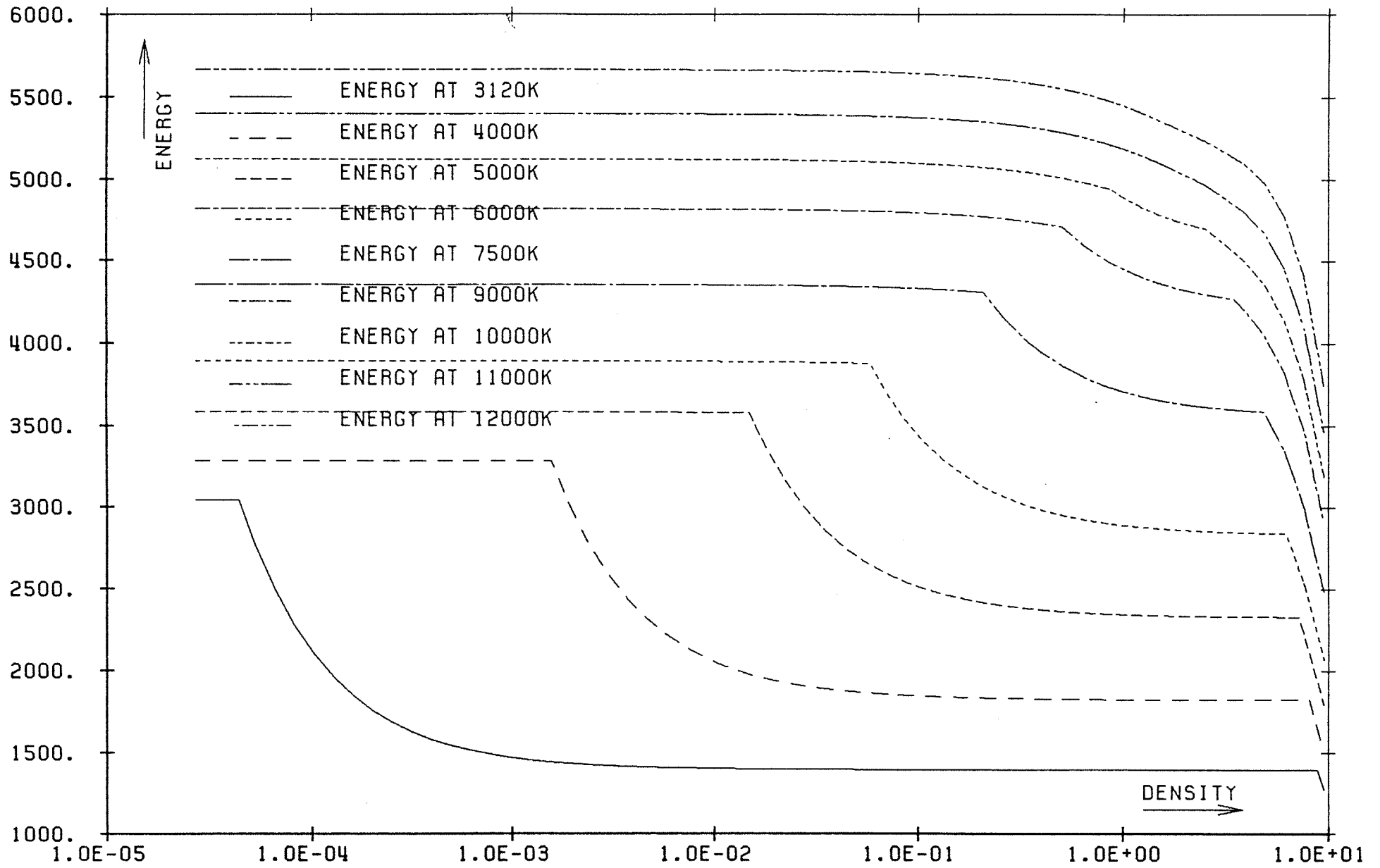


Fig.1 Internal Energy (J/g) versus Density (g/cm**3)

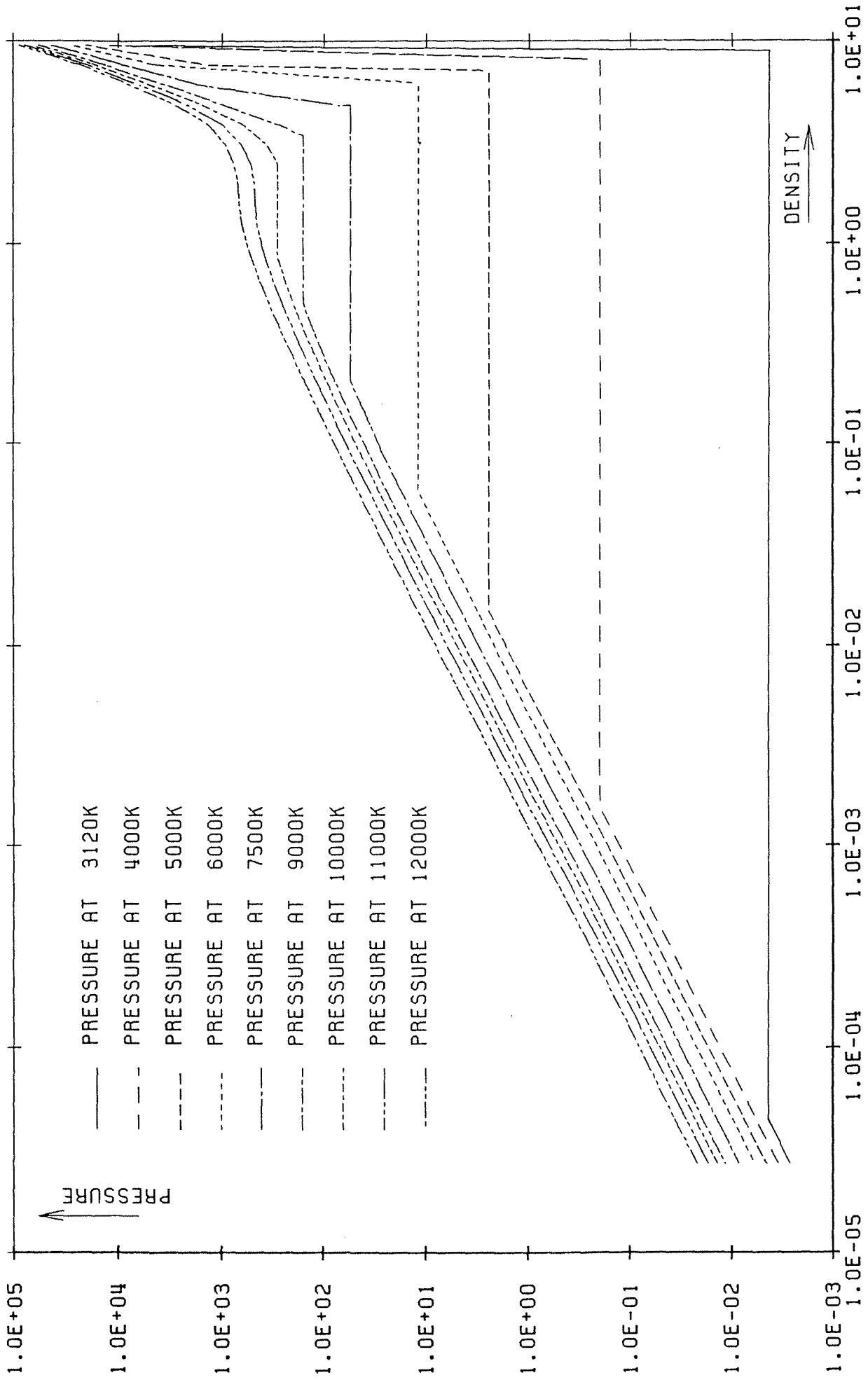


Fig.2 Total Pressure (Mpa) versus Density (g/cm**3)

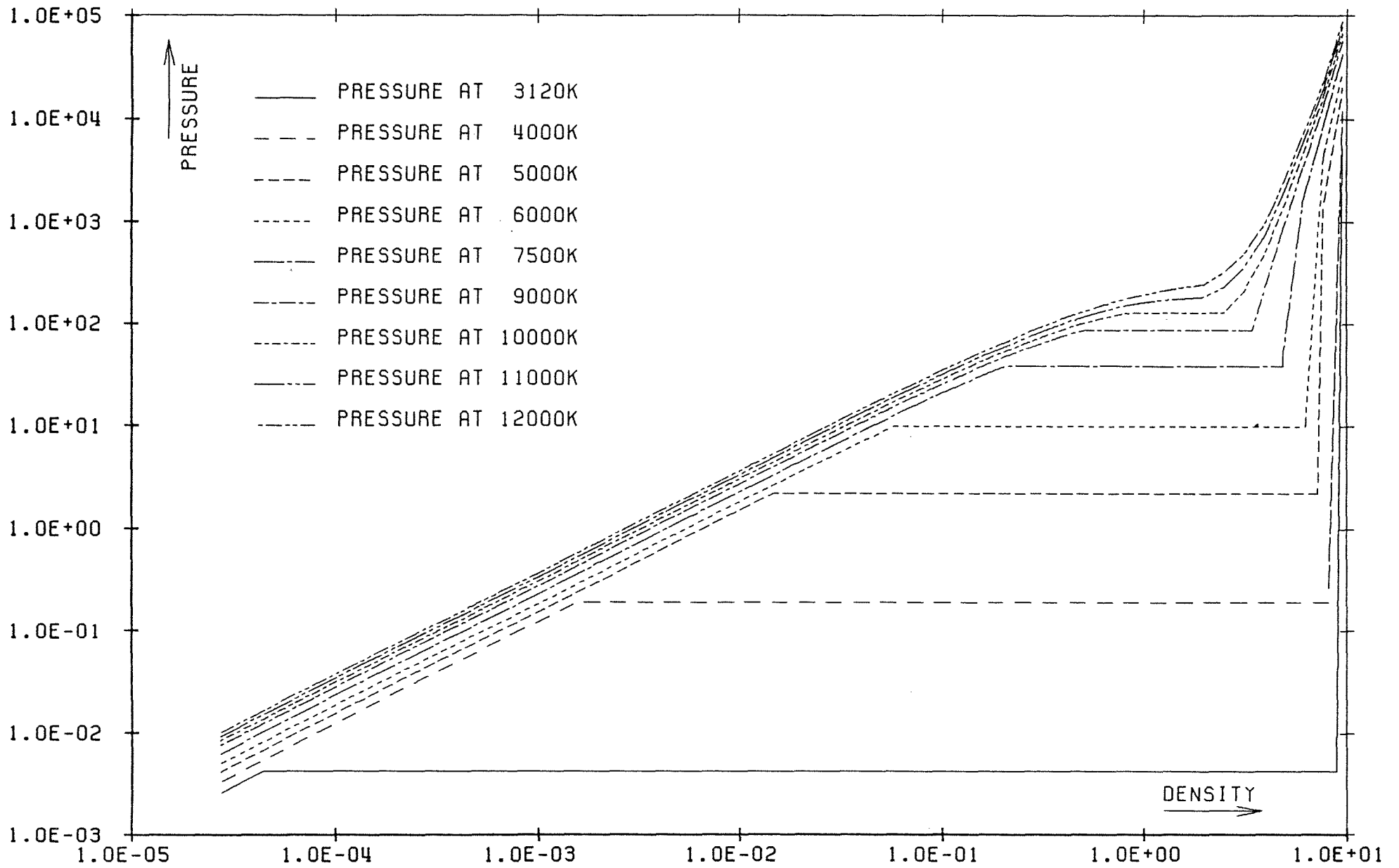


Fig.3 Saturation Pressure (Mpa) versus Density (g/cm^{**3})

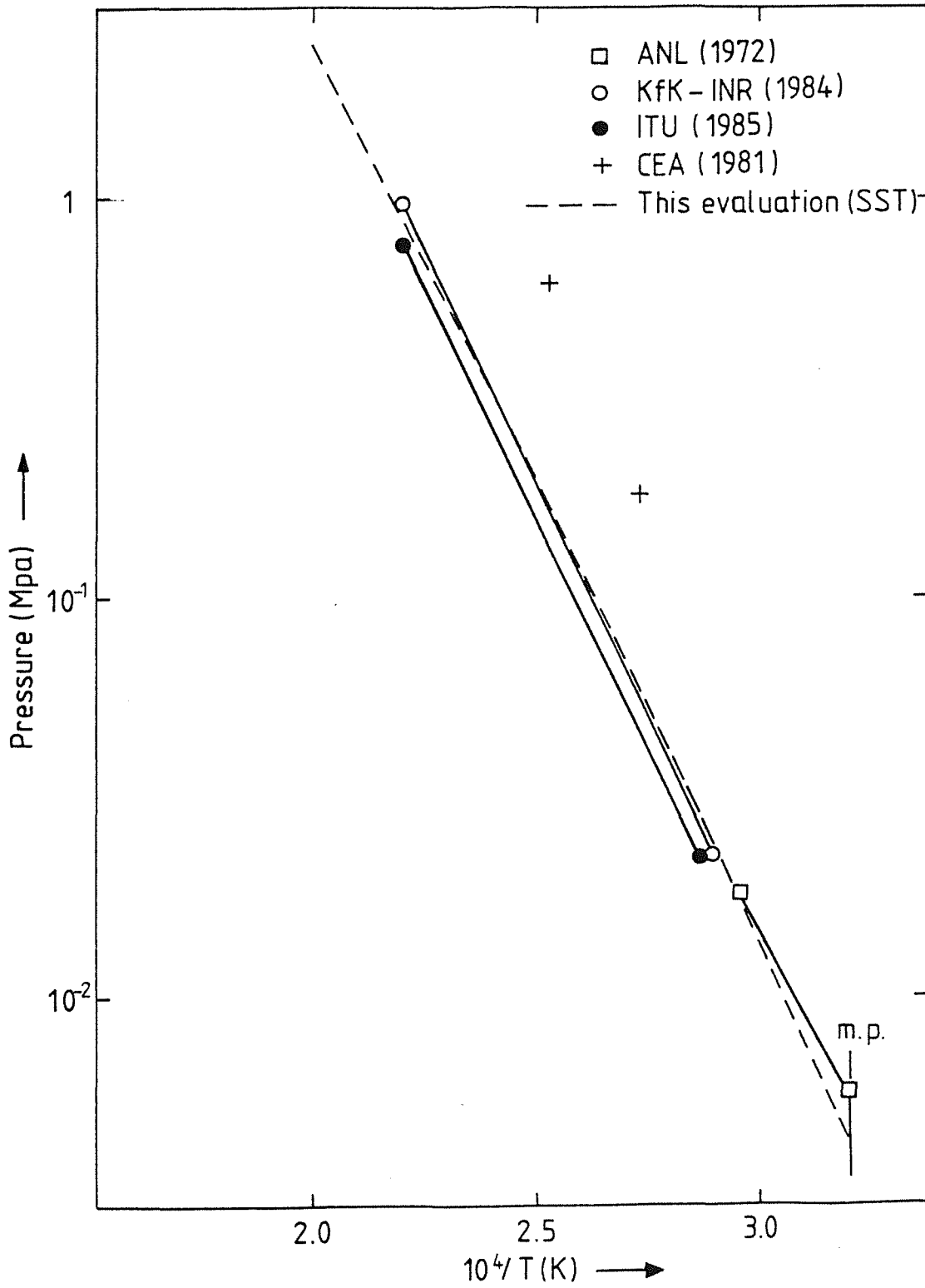


Fig.4: Total Pressure over Liquid UO_2
Versus Inverse Temperature (m.p.= melting point)

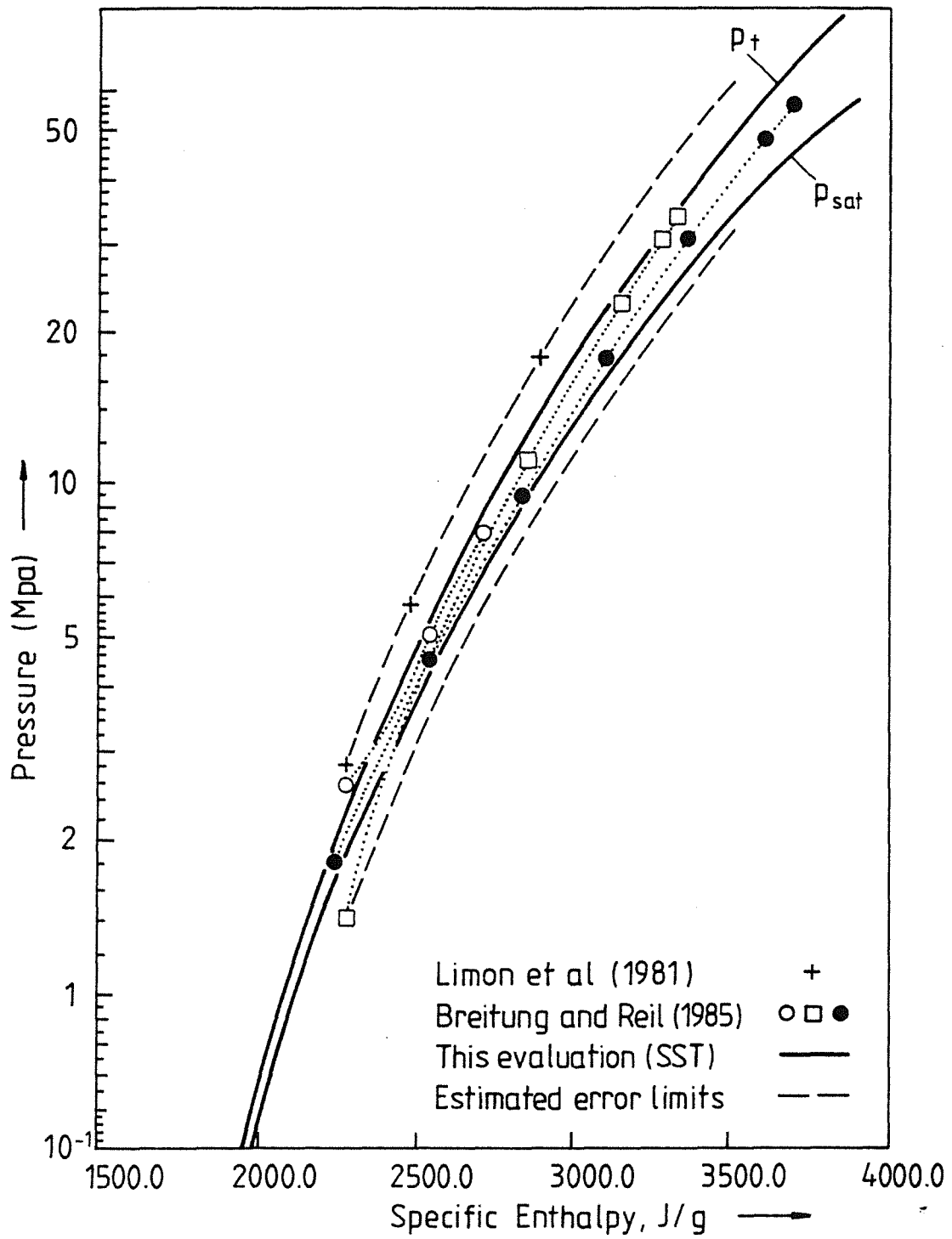


Fig.5: Vapor Pressure over Liquid UO_2 Versus Specific Enthalpy

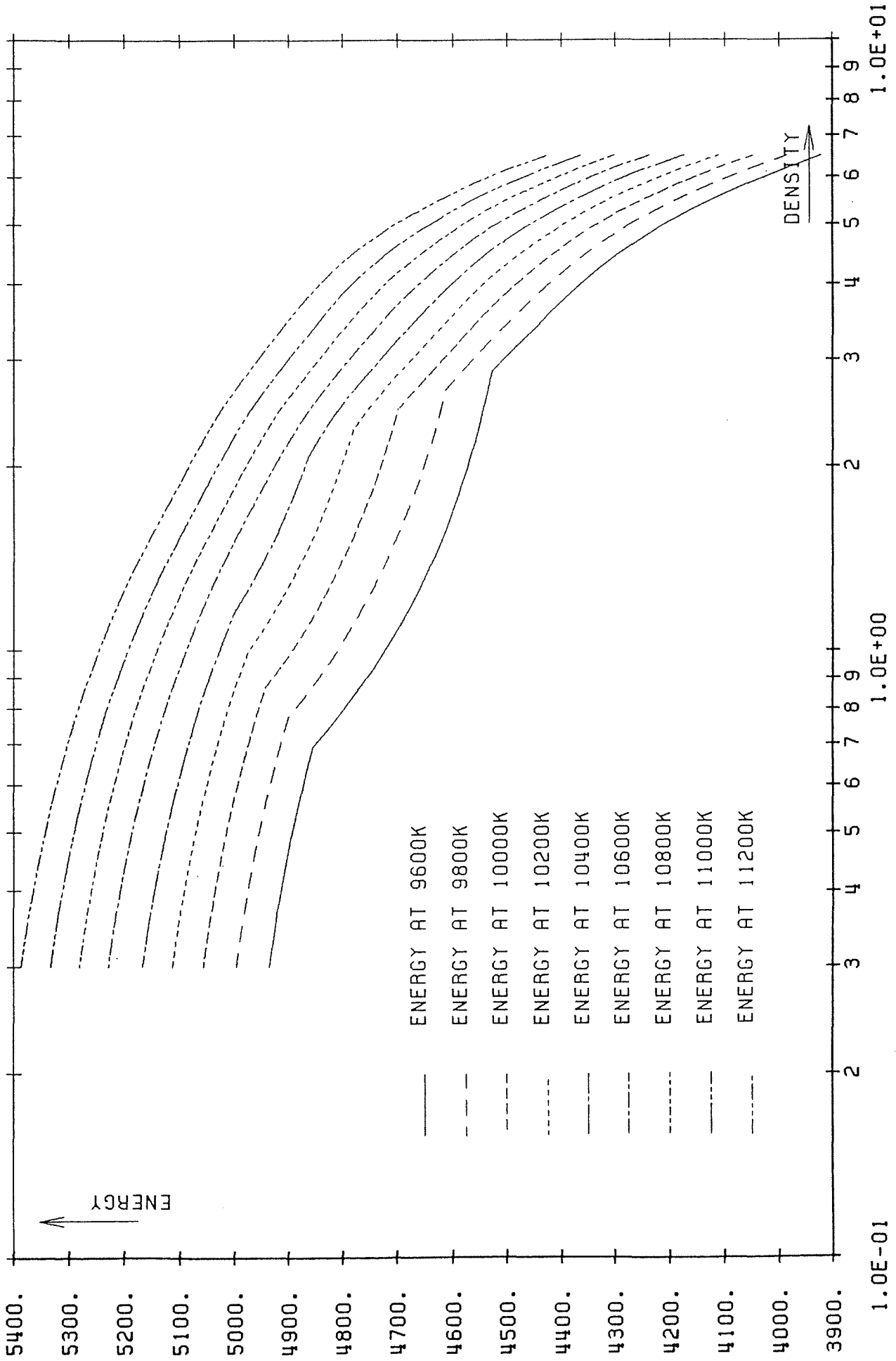


Fig.6 Internal Energy (J/g) vs Density (g/cm**3) near Critical Point

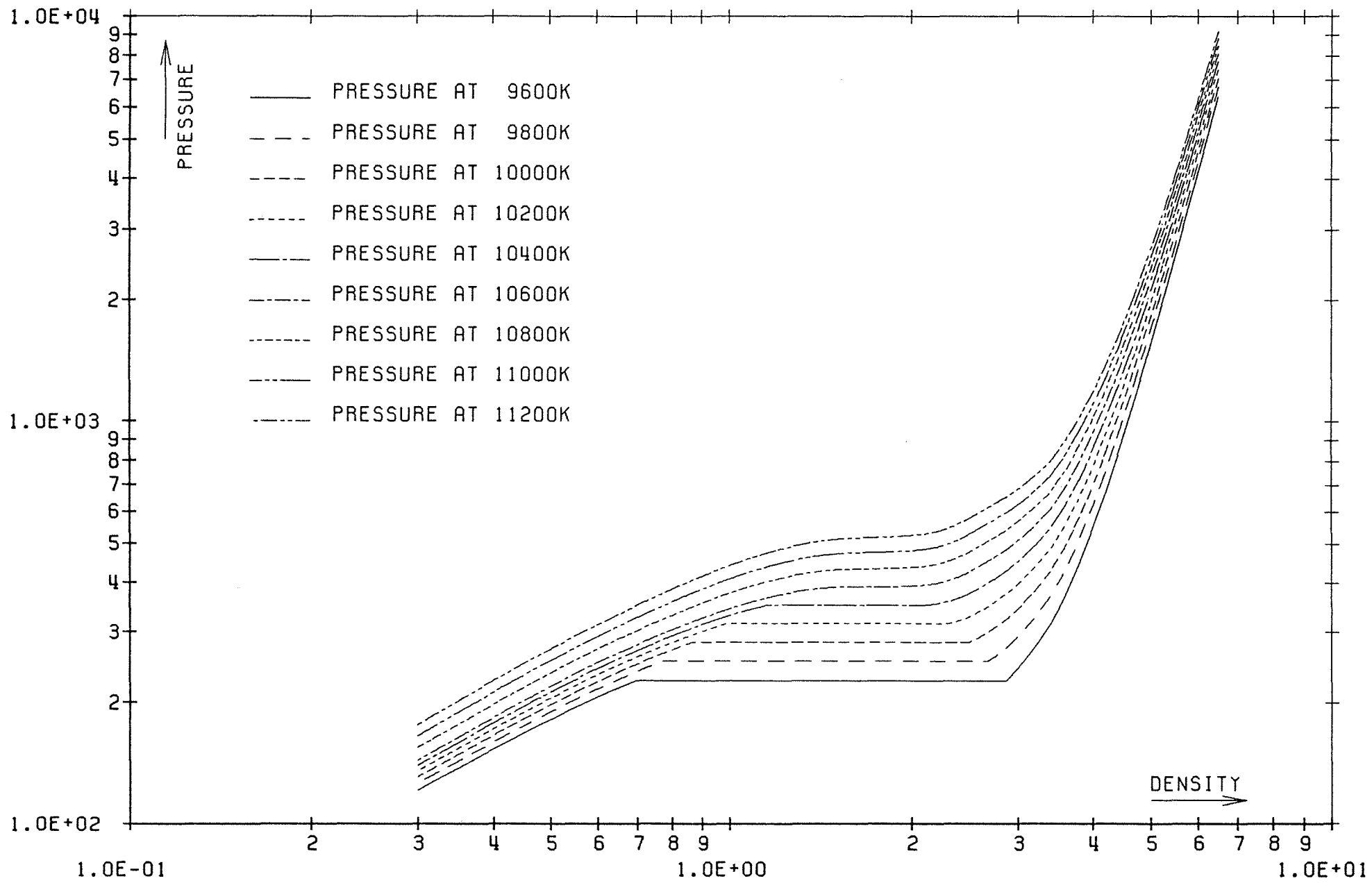


Fig.7 Total Pressure (Mpa) vs Density (g/cm**3) near Critical Point

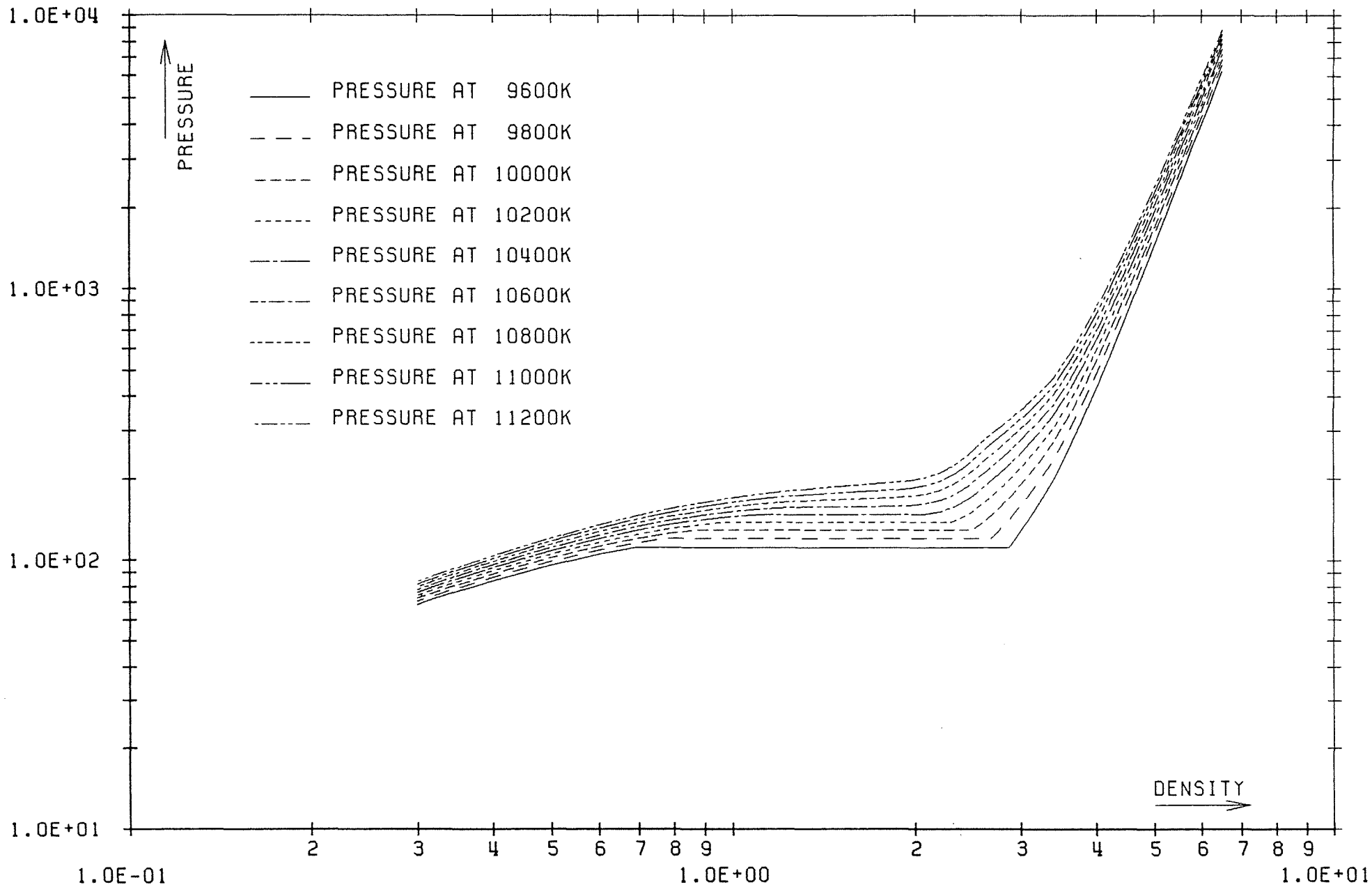


Fig.8 Satur. Pressure (Mpa) vs Density (g/cm³) near Critical Point

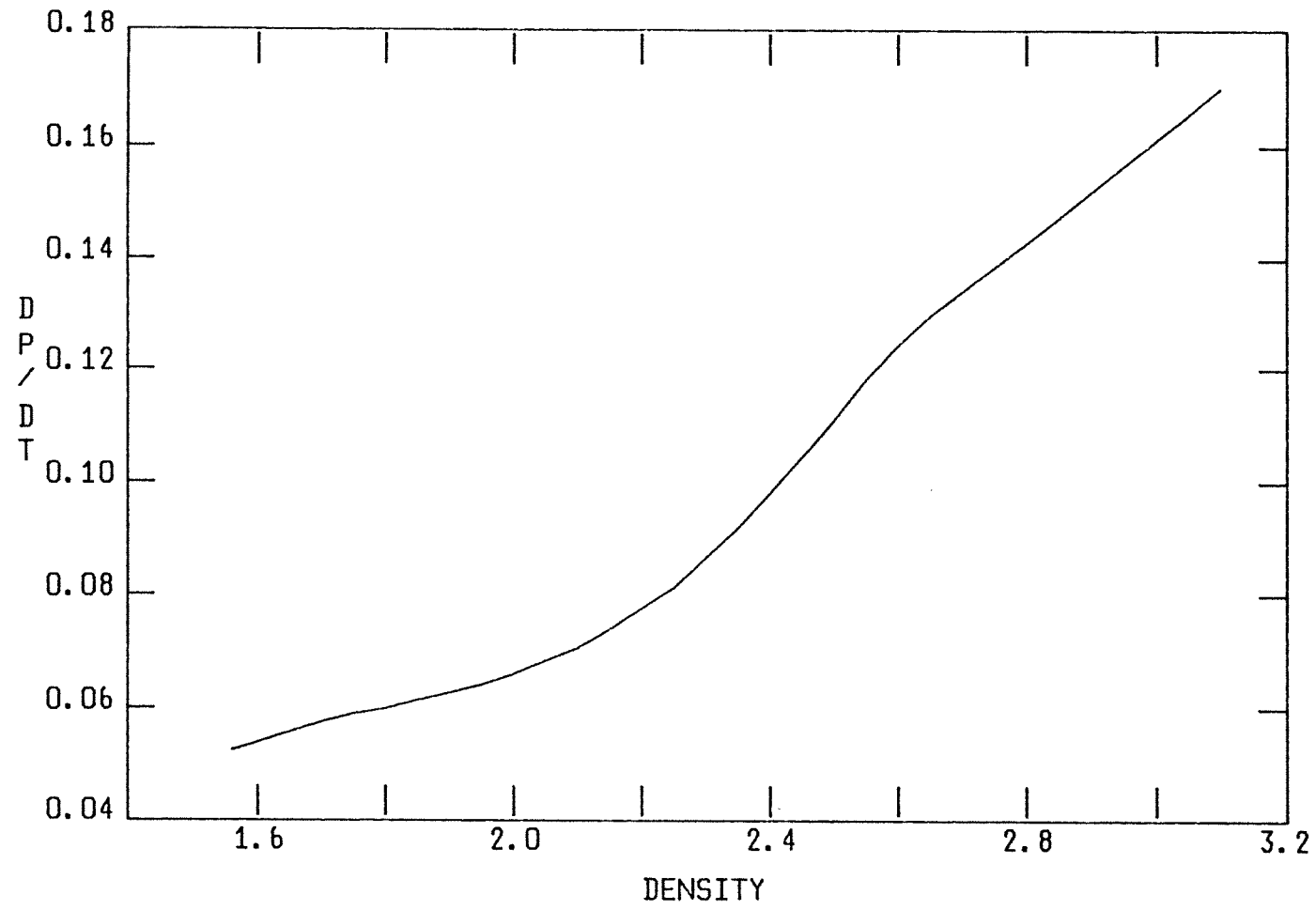


Fig.9 $\frac{dp}{dT}$ (Mpa/K) vs Density (g/cm^3)